

Ubiquitin Proteasome System Stress Underlies Synergistic Killing of Ovarian Cancer Cells by Bortezomib and a Novel HDAC6 Inhibitor

Martina Bazzaro,¹ Zhenhua Lin,¹ Antonio Santillan,^{1,2} Michael K. Lee,¹ Mei-Cheng Wang,³ Kwun C. Chan,³ Robert E. Bristow,² Ralph Mazitschek,⁴ James Bradner,^{4,5} and Richard B.S. Roden^{1,2}

Abstract Purpose: Elevated metabolic activity of ovarian cancer cells causes increased ubiquitin-proteasome-system (UPS) stress, resulting in their greater sensitivity to the toxic effects of proteasomal inhibition. The proteasomes and a potentially compensatory histone deacetylase 6 (HDAC6)-dependent lysosomal pathway mediate eukaryotic protein turnover. We hypothesized that up-regulation of the HDAC6-dependent lysosomal pathway occurs in response to UPS stress and proteasomal inhibition, and thus, ovarian cancer cell death can be triggered most effectively by coinhibition of both the proteasome- and HDAC6-dependent protein degradation pathways.

Experimental Design: To address this hypothesis, we examined HDAC6 expression patterns in normal and cancerous ovarian tissues and used a novel HDAC6-specific inhibitor, NK84, to address HDAC6 function in ovarian cancer.

Results: Abnormally high levels of HDAC6 are expressed by ovarian cancer cells *in situ* and in culture relative to benign epithelium and immortalized ovarian surface epithelium, respectively. Specific HDAC6 inhibition acts in synergy with the proteasome inhibitor Bortezomib (PS-341) to cause selective apoptotic cell death of ovarian cancer cells at doses that do not cause significant toxicity when used individually. Levels of UPS stress regulate the sensitivity of ovarian cancer cells to proteasome/HDAC6 inhibition. Pharmacologic inhibition of HDAC6 also reduces ovarian cancer cell spreading and migration consistent with its known function in regulating microtubule polymerization via deacetylation of α -tubulin.

Conclusion: Our results suggest the elevation of both the proteasomal and alternate HDAC6-dependent proteolytic pathways in ovarian cancer and the potential of combined inhibition of proteasome and HDAC6 as a therapy for ovarian cancer.

The ubiquitin-proteasome-system (UPS) and the histone deacetylase 6 (HDAC6)-dependent lysosomal pathway are two major pathways for protein turnover within eukaryotic cells (1). The proteasome inhibitor Bortezomib (PS-341) has recently been licensed for the treatment of refractory multiple myeloma and mantle cell lymphoma, and it is currently being

examined as a treatment for several cancer types including ovarian carcinoma (2–4). PS-341 exhibits selective antitumor activity against ovarian cancer cells *in vitro*, but in a xenograft model, it only slowed ovarian tumor growth (5). Accumulating evidence suggests that the lysosomal pathway can compensate for intracellular poly-ubiquitinated protein degradation when UPS activity is insufficient (6–9). A critical component of the lysosomal protein degradation pathway is a microtubule-associated deacetylase, HDAC6 activities, which directly interacts with misfolded and/or poly-ubiquitinated proteins to target them for lysosome-mediated protein degradation via aggresome formation/autophagy (10–12). Because misfolded and ubiquitinated proteins are degraded via both proteasomes and HDAC6-dependent autophagy, simultaneous inhibition of proteasome and HDAC6 activities has been proposed as a new strategy to synergistically induce cell death in multiple myeloma and pancreatic cancer settings (6, 13). Because we previously found that ovarian cancer cells exhibit significant UPS stress (5), here we examine the potential of inhibiting both the proteasomal and HDAC6-dependent protein degradation pathways as new approach for ovarian cancer treatment. Herein, we show that ovarian cancer cells are selectively sensitive to combined inhibition of proteasome and HDAC6-dependent protein degradation pathways and the potential of this approach for treatment of ovarian cancer.

Authors' Affiliations: Departments of ¹Pathology, ²Oncology, Obstetrics and Gynecology, and ³Biostatistics, The Johns Hopkins University, Baltimore, Maryland; and ⁴The Broad Institute of Harvard and MIT, Cambridge, Massachusetts, and Department of Biological Chemistry and Molecular Pharmacology, Harvard Medical School and ⁵Division of Hematologic Neoplasia, Dana-Farber Cancer Institute, Boston, Massachusetts
Received 3/11/08; revised 6/24/08; accepted 6/25/08.

Grant support: US Public Health Service grants R01CA122581 (R.B.S. Roden), P50 CA098252 (R.B.S. Roden, R.E. Bristow, and M.C. Wang), and the HERA foundation (M. Bazzaro, Z. Lin, and A. Santillan).

The costs of publication of this article were defrayed in part by the payment of page charges. This article must therefore be hereby marked *advertisement* in accordance with 18 U.S.C. Section 1734 solely to indicate this fact.

Note: Supplementary data for this article are available at Clinical Cancer Research Online (<http://clincancerres.aacrjournals.org/>).

Requests for reprints: Richard Roden, Johns Hopkins University, Cancer Research Building 2, Room 308, 1550 Orleans Street, Baltimore, MD 21231. Phone: 410-502-5161; Fax: 443-287-4295; E-mail: roden@jhmi.edu.

©2008 American Association for Cancer Research.
doi:10.1158/1078-0432.CCR-08-0642

Translational Relevance

We show that levels of ubiquitin-proteasome-system stress regulate the sensitivity of ovarian cancer cells to combined inhibition of HDAC6 with a novel compound and proteasome function with a licensed agent, Bortezomib/PS-341. We also show that inhibition of HDAC6, which is known to regulate tubulin acetylation and microtubule polymerization, reduces ovarian cancer cell spreading and migration. Our results support the development of combined inhibition of proteasome and HDAC6 as a therapy for ovarian cancer. Our findings are significant because of the novel mechanistic insights into the aberrant regulation of HDAC6 and the proteolytic machinery in ovarian cancer, and the potential value of inhibitors in these pathways as a new approach that is urgently needed to treat ovarian cancer patients.

Materials and Methods

Human specimens and cell lines. Studies using human tissue were done with the approval of the Johns Hopkins Institutional Review Board. Fresh and archival tissues were obtained from the Department of Pathology of the Johns Hopkins Hospital and the latter assembled in tissue microarrays by a core facility. IOSE-29 and IOSE-397 were kindly provided by Nelly Auesperg (University of British Columbia, Vancouver, British Columbia, Canada) and cultured in Medium 199 and MCDB105 (1:1) with 10% fetal bovine serum and 50 µg/mL gentamicin (Invitrogen). SKOV-3 and ES-2 and TOV-21G were obtained from American Type Culture Collection and cultured in DMEM containing 10% fetal bovine serum and 50 µg/mL gentamicin (Invitrogen).

Preparation of bone marrow samples and isolation of CD34+ cells. Bone marrow aspirate was obtained from individuals who gave written informed consent in accordance with the Johns Hopkins Institutional Review Board. Under sterile conditions, samples were processed through Ficoll-density gradient for isolation of mononuclear cells as described previously (14). To purify CD34+ cells, mononuclear cells were resuspended in 500 µL of binding buffer containing PBS+0.5% bovine serum albumin. The cell suspension was incubated with 100 µL of human CD34 MicroBeads (Miltenyi Biotech), for 30 min at 4°C. After incubation, the cells were washed and processed through a MACS magnetic separator column (Miltenyi Biotech). Cells labeled with microbeads were passed through a column placed in a magnetic field and the target cells retained. After washing the column, the target cells were recovered by removing the magnetic field and flushing the column with PBS+0.5% BSA. Recovered cells were resuspended in DMEM containing 10% fetal bovine serum, and their viability was evaluated by trypan blue dye exclusion.

Immunohistochemistry of tissue microarrays. Immunohistochemical analysis of paraffin-embedded tissues was done as previously described (5). Staining was diffuse across the cancer tissues and therefore was scored only on the basis of intensity. The staining was scored by three observers blind to specimen identity to obtain a consensus. Staining intensity was scored as negative (0), weak (1), intermediate (2), or strong (3).

Reagents. The proteasome inhibitor PS-341 was provided by Millenium Pharmaceuticals, Inc. The HDAC6-specific inhibitors Tubacin and NK84 were obtained from the Broad Institute and the Massachusetts Institute of Technology. Cycloheximide was purchased from Sigma Aldrich.

Antibodies and Western blot analysis. Total cellular protein (10–20 µg) from each sample was subjected to standard Western blot analysis. Antibodies were obtained from the following vendors: anti-HDAC6

(Cell Signaling), anti-ubiquitin and anti-vimentin (Santa Cruz Biotechnology), anti-β-actin (Sigma), anti-PARP (BD Biosciences), anti-Hsp90 (StressGene), anti-acetyl-lysine (Cell Signaling), anti-cortactin and anti-acetyl-α-tubulin (Abcam), peroxidase-linked anti-rabbit or anti-mouse Immunoglobulin G (Amersham), Texas red-labeled goat anti-mouse Immunoglobulin G (Molecular Probes), and Fluorescein-labeled horse anti-rabbit Immunoglobulin G (Vector Laboratories). Antibodies were used at the concentration recommended by the manufacturer.

Immunoprecipitation of Hsp90 or cortactin and immunoblot analyses. ES-2 ovarian cancer cells treated or not with Tubacin or NK84 were lysed in radioimmunoprecipitation assay buffer (Thermo Scientific) containing complete protease inhibitor cocktail (Roche) for 15 min on ice and subsequently centrifuged to remove nuclear and cellular debris. Two hundred micrograms of cell lysates were incubated with Hsp90 or Cortactin specific monoclonal antibodies for 1 h at 4°C. The protein G-agarose beads were added and the mixture incubated at 4°C overnight. The immunoprecipitates were washed and the proteins eluted with SDS sample loading buffer prior immunoblot analysis with specific antibodies against Hsp90, Cortactin, and Acetyl-Lysine (15, 16).

2,3-Bis[2-methoxy-4-nitro-5-sulphophenyl]-2H-tetrazolium-5-carboxanilide inner salt assay. Cell viability/proliferation was determined by 2,3-bis-[2-methoxy-4-nitro-5-sulphophenyl]-2H-tetrazolium-5-carboxanilide inner salt (XTT) assay (Roche Diagnostics GmbH) as previously described (5). All the experiments were done in triplicate.

Histone deacetylase biochemical assay. To measure the inhibitory effect on HDAC6 function *in vitro*, an optimized, continuous kinetic biochemical assay was used. Purified, full-length HDAC protein (HDAC1, 3.33 ng/µL; HDAC2, 1 ng/µL; HDAC3/NCOR2, 0.17 ng/µL; HDAC6 1.3 ng/µL; BPS Biosciences) was incubated with a commercially available fluorophore-conjugated substrate at a concentration equivalent to the substrate K_m (Upstate 17-372; 6 µmol/L for HDAC1, 3 µmol/L for HDAC2, 6 µmol/L for HDAC3, and 16 µmol/L for HDAC6). Reactions were done in assay buffer [50 mmol/L HEPES, 100 mmol/L KCl, 0.001% Tween 20, 0.05% BSA (pH 7.4)] and followed for fluorogenic release of 7-amino-4-methylcoumarin from substrate upon deacetylase and trypsin enzymatic activity. Fluorescence measurements are obtained as replicates in real-time on a Varioskan microtiter plate reader (Thermo). Calculation of K_i is determined using a derivation of the standard formula $K_i = [Inhibitor]/((V/V_0) * (1 + S/K_m)) - ([Substrate]/K_m) - 1$.

In vitro cell spreading and migration assays. SKOV-3 confluent cultures were scratched by using a sterile pipette tip and examined by phase-contrast microscopy with Spot 3.5.8 acquisition software. For migration chamber assay (2.5×10^4) SKOV-3 or ES-2 mock-treated or NK84-treated cells were seeded in the upper well of a 24-well transwell migration chamber (Costar) previously coated with Matrigel. Higher serum concentration was added to the lower well as chemoattractant. Eight hours after seeding, the filter separating the chambers was removed and its upper surface swabbed to remove Matrigel and nonmigrating cells. The migrating cells on the lower surface of the membrane migration chambers were fixed and stained with H&E and counted. Each assay was done in triplicate.

Immuno-fluorescence analysis. For analysis of HDAC6, ubiquitin, and vimentin subcellular localization, cultures of SKOV-3, IOSE-29, and ES-2 were grown as described in Lab-Tek II chambered cover glass (Nalge Nunc International). At the indicated times, cells were fixed and permeabilized with methanol and incubated with the indicated primary antibodies. Fluorescent secondary antibodies were used to visualize protein localization, and nuclei were visualized by 4,6-diamidino-2-phenylindole staining. Mounted samples were viewed under a Nikon Eclipse TE 2000E inverted microscope and images captured with Spot 3.5.8 acquisition software (Diagnostic Instruments).

Statistical analysis. Results are reported as mean ± SD. Unless otherwise indicated, statistical significance of difference was assessed by two-tailed Student's *t* using Prism (V.4 Graphpad) and Excel. The level of significance was set at a *P* value of <0.05. The combination index of PS-341 and Tubacin was calculated by the method of Chou and Talalay (17).

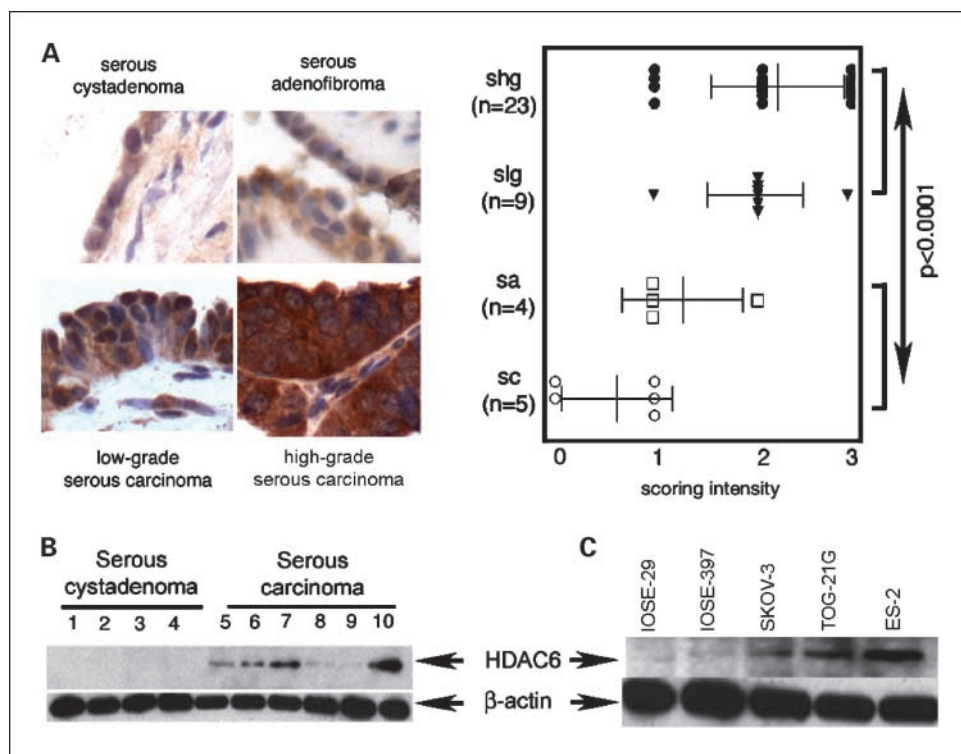


Fig. 1. HDAC6 overexpression in ovarian carcinoma and cell lines. **A**, immunohistochemical staining of HDAC6 in ovarian tumors (*left*). Representative examples of intense HDAC6 staining of high-grade and low-grade ovarian serous carcinomas and weaker staining in serous adenofibroma and serous cystadenoma (objective, $\times 40$; *right*) staining intensity for each case was graded as 0 (no staining), 1 (weak staining), 2 (moderate staining), and 3 (intense staining), and the statistical significance of differences in staining intensities among indicated groups was calculated using the Mann-Whitney *U* test. *Error bars*, SD. **B**, Western blot analysis of HDAC6 in clinical specimens of serous cystadenoma (*lanes 1-4*) and serous carcinoma (*lanes 5-10*). Equal loading was verified by using an antibody directed against β -actin. **C**, Western blot analysis of HDAC6 immortalized ovarian surface epithelial cells (IOSE-29 and IOSE-397) and ovarian cancer cell lines (SKOV-3, ES-2, and TOV-21G). Equal protein loading in each lane was verified by using an antibody directed against β -actin.

Results

HDAC6 overexpression in ovarian cancer cells and tissues. To determine whether HDAC6 expression is altered in ovarian carcinogenesis, we assessed HDAC6 expression patterns in benign ovarian lesions and ovarian serous carcinoma by semiquantitative immunohistochemical staining of tissue microarrays. HDAC6 expression levels were higher in low-grade and high-grade ovarian carcinomas compared with benign lesions (serous cystadenoma and serous adenofibroma; Fig. 1A). Consistent with the immunohistochemical study, immunoblot analysis shows higher levels of HDAC6 in ovarian carcinomas than the benign cystadenoma (Fig. 1B). HDAC6 levels were assessed in a panel of ovarian cancer cell lines (SKOV-3, TOV-21G, and ES-2) and in immortalized ovarian surface epithelial cell lines (IOSE-29 and IOSE-397). Consistent with the *in vivo* profile of HDAC6 overexpression, the ovarian cancer cell lines tested showed consistently higher levels of HDAC6 compared with IOSE cell lines (Fig. 1C).

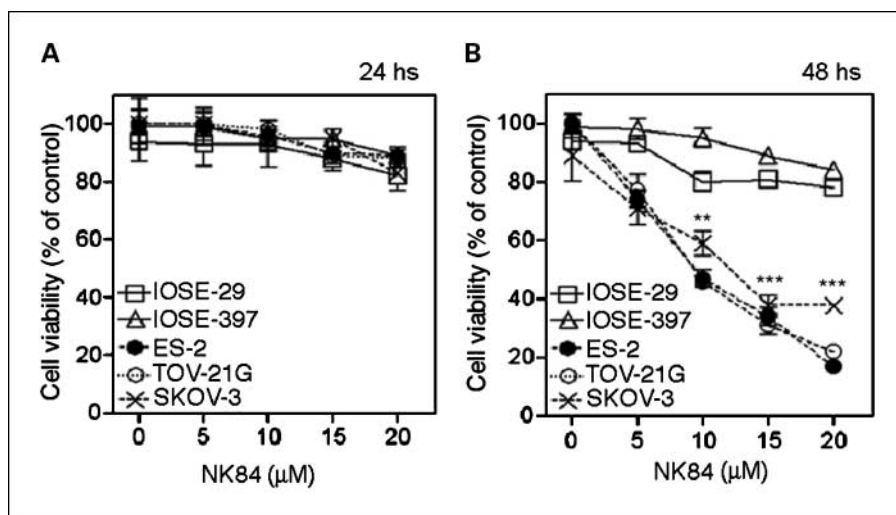
HDAC6 inhibition specifically inhibits growth of ovarian cancer cells in vitro. We recently reported (5) that overexpression of proteasomes in ovarian cancer correlates with increased sensitivity of ovarian cancer cells to the proteasome inhibitor PS-341. Given our observation of increased HDAC6 expression in ovarian cancer cells, we examined if HDAC6 activity is important for normal growth/survival of ovarian cancer cells by comparing the relative sensitivity of a panel of ovarian cancer cell lines (SKOV-3, TOV-21G, and ES-2) and IOSE cell lines to selective 1,3-dioxane-based HDAC6 inhibitors, Tubacin (6), and NK84 (18). Tubacin and NK84 are potent inhibitors of HDAC6 (HDAC6 K_i 20 and 2.5 $\mu\text{mol/L}$, respectively), which show a 10-fold to >100-fold window of selectivity over other class I and class II

deacetylases.⁶ Although minimal cell death is observable after 24 hours of NK84 treatment in all cell lines (Fig. 2A), 48 hours of NK84 treatment severely compromised the viability of ovarian cancer cell lines in a dose-dependent fashion sparing the immortalized counterpart (Fig. 2B). Similar results were obtained when using the previously characterized HDAC6 specific inhibitor Tubacin (Supplementary Fig. S1). The toxicity profile of NK84 and Tubacin for ovarian cancer cells is consistent with their greater dependence upon HDAC6 activity.

Synergistic killing of ovarian cancer cells by NK84 and PS-341. The up-regulation of both proteasome and HDAC6 in ovarian cancer, together with the selective cytotoxicity of individual treatment with either proteasome or HDAC6 inhibitors, suggested that combined inhibition of both proteasome and HDAC6-assisted proteolytic pathways might represent an effective treatment for ovarian carcinoma. To test this hypothesis, we compared the effects of combined treatment with PS-341 and NK84 on a panel of ovarian cancer cell lines and IOSEs. Figure 3A and B show that submaximal doses of inhibitors act synergistically to cause dramatic cytotoxicity in the ovarian cancer cells (ES-2 and TOV-21G). Combination indices of 0.3 and 0.5 were observed when combining 10 $\mu\text{mol/L}$ NK84 with either 5 or 10 nmol/L of PS-341, respectively (17). Similar data were obtained with the several ovarian cancer cell lines we tested (data not shown) and also using the HDAC6-specific inhibitor Tubacin. Significantly, the cytotoxicity achieved using the combination of individually nontoxic doses of PS-341 (5 nmol/L) and NK84 (5 $\mu\text{mol/L}$) was comparable with that achieved with the highest dose of PS-341 or PS-341/NK84 in combination. This apparent saturation of cytotoxicity suggests that both

⁶ J.E. Bradner and R. Mazitschek, unpublished data.

Fig. 2. NK84 treatment reduces the viability ovarian cancer cells while sparing IOSEs. *A*, ovarian cancer cell lines (SKOV-3, ES-2, and TOV-21G) and immortalized ovarian surface epithelial cells (IOSE-29 and IOSE-397) were treated with the HDAC6 inhibitor NK84 (*A* and *B*) at the concentrations indicated. Cell viability was measured by XTT assay after culturing the cells for 24 h (*A*) or 48 h (*B*) in presence of NK84 inhibitor. Points, mean; bars, SD.



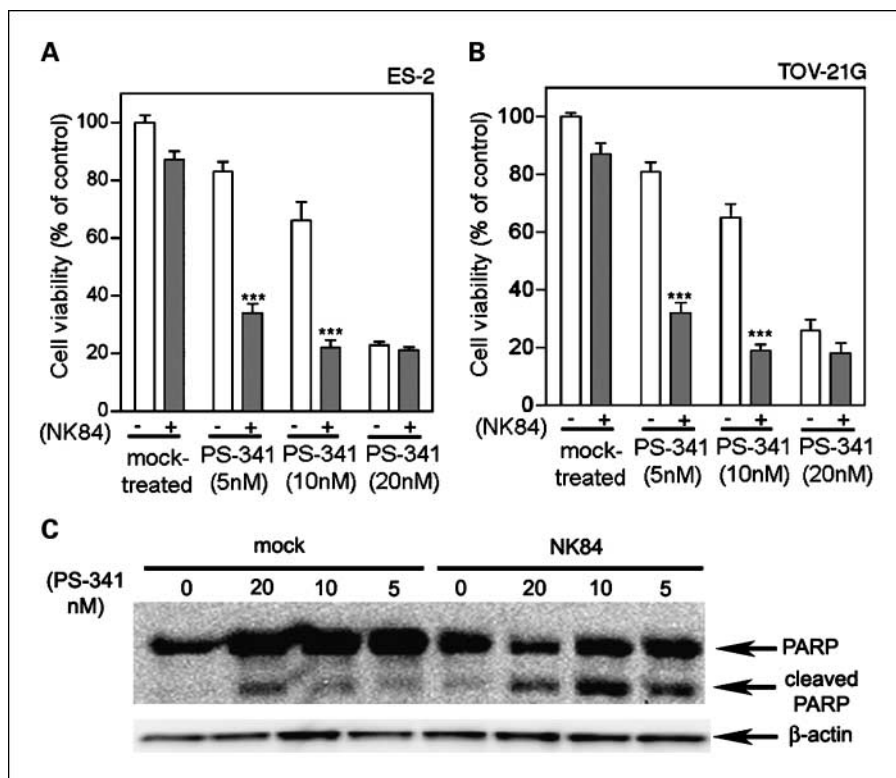
compounds are acting on the same pathway to cause cell death. In contrast to the results with cancer cells, the combination of PS-341 and NK84 does not affect cell viability of either non-tumorigenic IOSE cell lines or CD34+ bone marrow-derived progenitor cells (Supplementary Fig. S2), indicating a potential host sparing effect of HDAC6/proteasome combination.

NK84 is a derivative of the previously identified HDAC6-specific inhibitor Tubacin. To provide direct evidence that NK84 specifically inhibits HDAC6, we show that NK84 treatment induces α -tubulin hyperacetylation in cultured ovarian cancer cells (Supplementary Fig. S2A). Because cortactin and Hsp90 are additional known substrates for HDAC6 activity, we tested whether HDAC6 inhibition via Tubacin or NK84 treatment induces heat shock protein 90 and/or cortactin hyperacetylation in ovarian cancer cells.

Our data show no change in the levels of acetylated cortactin or Hsp90 after NK84 treatment (Supplementary Fig. S2B and C). These results are in line with previous reports (19, 20) indicating that although deacetylation of Hsp90 and cortactin is HDAC6-mediated, both Tubacin and NK85 only affect the α -tubulin deacetylase domain of HDAC6. As a further evidence that the synergistic effect upon PS-341/NK84 inhibition does not occur via Hsp90 hyperacetylation, we failed to observe synergy for the combination of PS-341 and the Hsp90 inhibitor Geldanamycin (21) for killing of ovarian cancer cell lines (data not shown).

To assess whether the loss of viability occurs via apoptosis, we measured the levels of PARP cleavage in ovarian cancer cells receiving NK84 and/or PS-341 treatment. As shown in Fig. 3C, high levels of cleaved PARP are apparent when using

Fig. 3. Simultaneous inhibition of HDAC6 and proteasome activity induces synergistic killing of ovarian cancer cells. Dose-dependent inhibition of the cell viability of ES-2 (*A*) and TOV-21G (*B*) in the absence (-) or in the presence (+) of 5 μ mol/L NK84 HDAC6 inhibitor and PS-341 at the indicated concentration. Cell viability was measured after a 24-h incubation by XTT assay and the percentage of viable cells is presented relative to mock-treated controls. ***, $P < 0.001$. Columns, mean; bars, SD. Lysate of ES-2 cell line treated with NK84 (5 μ m) and/or PS-341 at the indicated concentrations was immunoblotted with an antibody recognizing the full-length and cleaved forms of PARP. Equal protein loading was verified by using an antibody directed against β -actin.



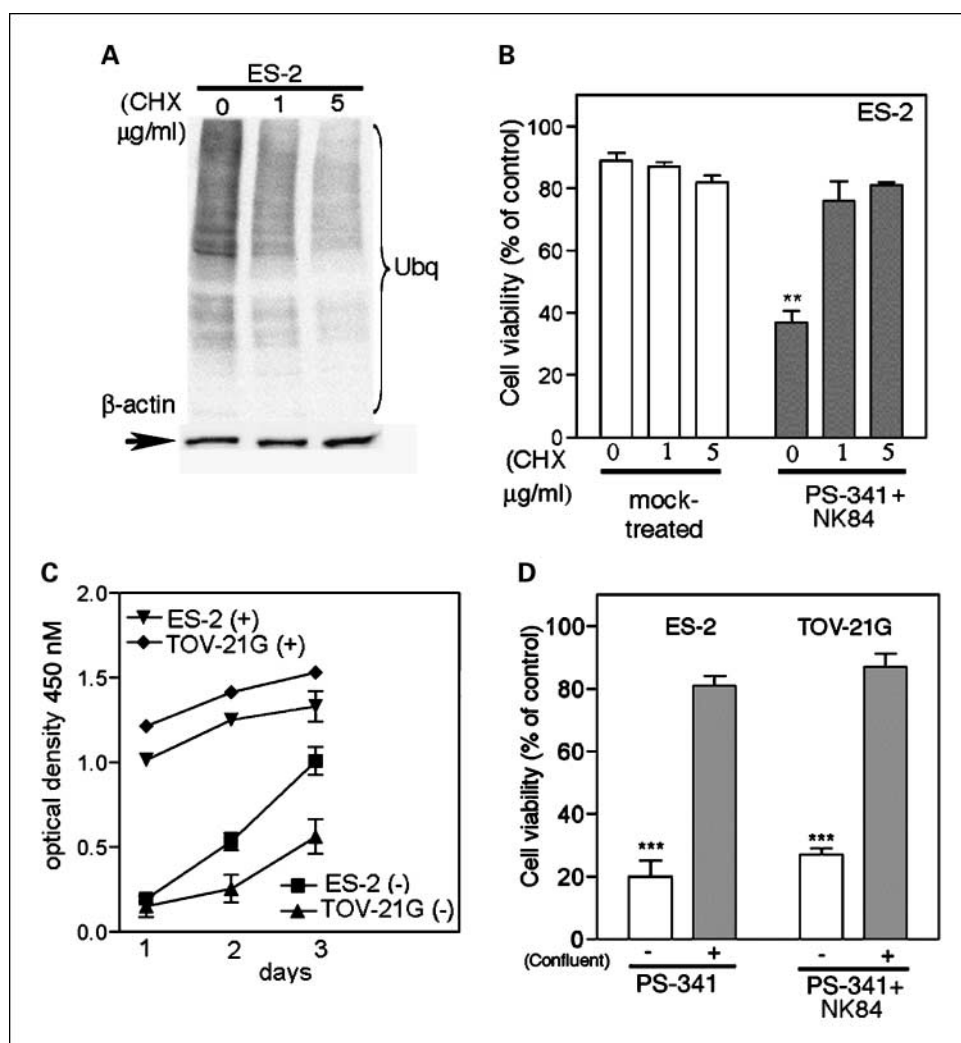


Fig. 4. Synergistic activity of PS-341 and NK84 on ovarian cancer cells is dependent on level of metabolic activity. *A*, immunoblot analysis of the levels of poly-ubiquitinated proteins in cyclohexamide-exposed (24 h) ES-2 ovarian cancer cells. Equal loading was verified by using an antibody directed against β -actin. *B*, ES-2 ovarian cancer cells pre-exposed to 0, 1 or 5 mg/mL cyclohexamide (CHX; 24 h) subsequently received treatment with of PS-341 (1 nmol/L) and NK84 (5 μ mol/L) or mock treatment. Cell viability was as evaluated by XTT assay after 24 h of treatment. Percentage of viable cells is relative to mock-treated control cells is presented. **, $P < 0.02$. Columns, mean; bars, SD. *C*, proliferation rate of confluent (+) or subconfluent (-) ES-2 and TOV-21G ovarian cancer cell lines was measured by XTT assay. Each assay was done in triplicate. Points, mean of proliferative activity measured in terms of absorbance at 450 nm on each given day; bars, SD. *D*, cell viability of ES-2 and TOV-21G ovarian cancer cell lines was evaluated by XTT assay in subconfluent (-) versus confluent (+) cultures in the presence of PS-341 1 nmol/L and NK84 5 μ mol/L. Percentage of viable cells is relative to mock-treated control cells. ***, $P < 0.001$. Columns, mean; bars, SD.

the combination of individually nontoxic doses of PS-341 (5 nmol/L) and NK84 (5 μ mol/L), indicating caspase-3 activation and the onset of apoptosis.

Synergy of NK84 and PS-341 is dependent on proliferation rate and UPS stress. We have shown that the sensitivity of ovarian cancer cells to PS-341 is dependent on their metabolic rate and degree of UPS stress (22). Thus, we reasoned that the requirement of ovarian cancer cell lines for proteasome and HDAC6 activity may also depend upon their levels of metabolic rate.

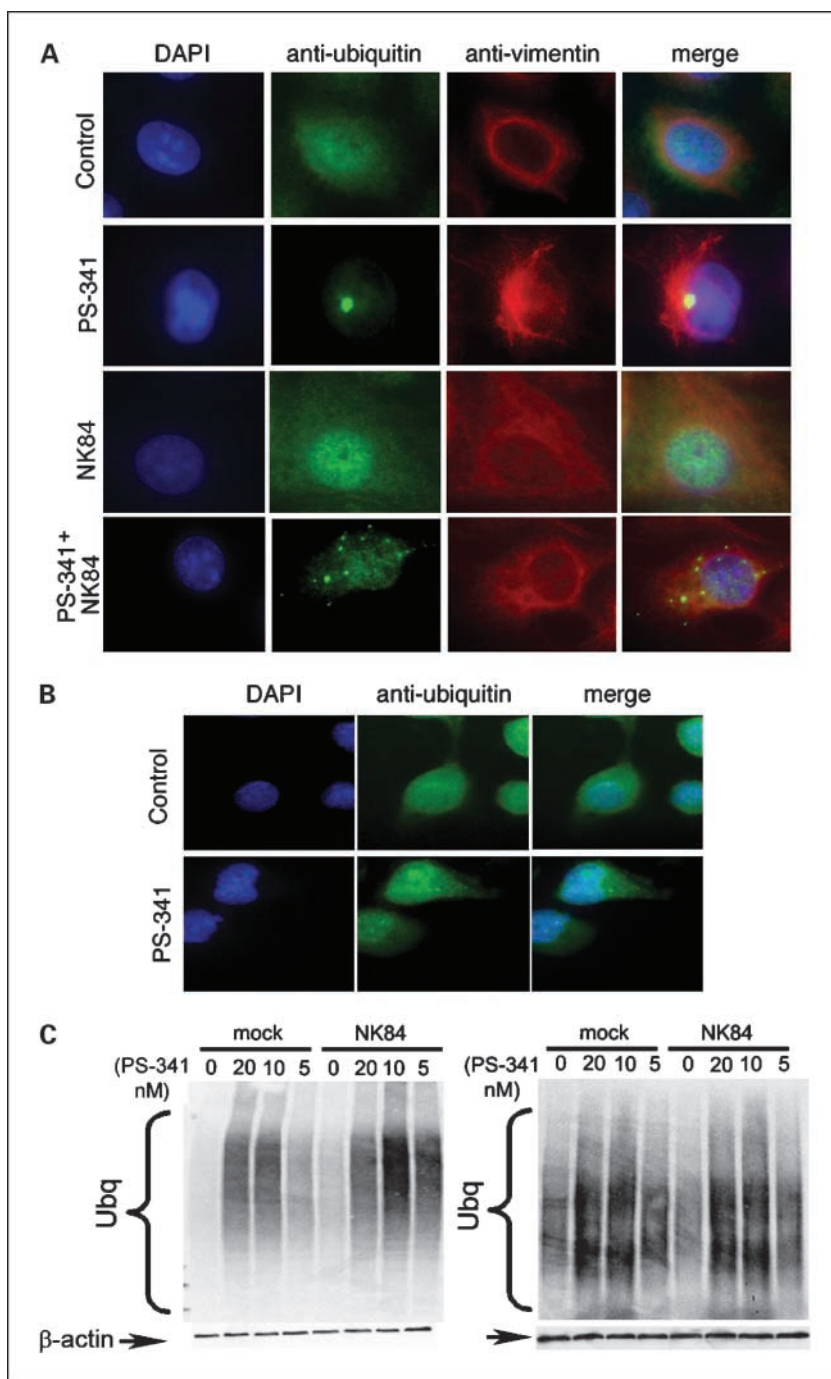
To test this hypothesis, ES-2 ovarian cancer cells were induced into quiescence by treatment with the translation inhibitor cyclohexamide. Cellular quiescence was accompanied with decrease of the UPS stress levels in cyclohexamide-treated cells versus control (Fig. 4A). Quiescent ES-2 ovarian cancer cell lines were tested for their sensitivity to the combination of PS-341 and NK84. The viability in cyclohexamide-treated cells was significantly higher compared with mock-treated cells, consistent with the hypothesis of a greater requirement of metabolically active cells for proteasome and HDCA6 activity (Fig. 4B). Because a decrease in proliferation rate of ovarian cancer cells is accompanied by a reduction in UPS stress (5), the proliferation of ES-2 and TOV-21G cells was slowed by contact-mediated growth inhibition (Fig. 4C), and their sensitivity to combination of NK84 and PS-341 treatment was

tested. Consistent with the hypothesis, NK84/PS-341 combination treatment severely compromised the viability of exponentially growing cells, while sparing contact-inhibited cell cultures (Fig. 4D).

Formation of aggresomes in response to UPS stress is prevented by NK84. Previously reported data suggest that the formation of aggresomes after proteasome inhibition is a cytoprotective event to limit proteasome inhibitor-induced cell death (13), whereas the cytotoxic effects of HDAC6 inhibition seems to be linked to inhibition of aggresome formation. Consistent with this view, immunofluorescence analysis of the poly-ubiquitinated proteins in ovarian cancer cells treated with a low, subtoxic dose of PS-341 (5 nmol/L) revealed the presence of vimentin-caged, ubiquitin-positive aggresomes in a half of the PS-341-treated cells. Conversely, simultaneous inhibition of both proteasome and HDAC6 function caused the appearance of poly-ubiquitinated proteins at multiple punctate sites throughout the cytoplasm (Fig. 5A). Interestingly, IOSEs failed to form aggresome-like structures even at the highest dose (20 nmol/L) of PS-341 (Fig. 5B).

We then examined the effect of proteasome and HDAC6 inhibition on accumulation of poly-ubiquitinated proteins by immunoblot analysis in ES-2 ovarian cancer cell and IOSE-29. Poly-ubiquitinated proteins accumulate in ES-2 cells upon

Fig. 5. HDAC6 inhibition prevents aggresome formation in UPS-stressed ovarian cancer cells. **A**, ES-2 ovarian cancer cells were incubated with 5 nmol/L PS-341, 10 μ mol/L NK84, or the combination of both for 24 h before fixation and immuno-fluorescent staining of DNA (*blue*), ubiquitin (*green*), and vimentin (*red*) and imaging (objective, $\times 60$). **B**, IOSE-29 cells were incubated with 20 nmol/L PS-341 for 24 h before fixation and immuno-fluorescent staining of DNA (*blue*), ubiquitin (*green*), and vimentin (*red*), and imaging (objective, $\times 60$). **C**, immunoblot analysis of ubiquitinated protein in ES-2 cells (*left*) or IOSE-29 cells (*right*) 24 h after treatment with or without 10 μ mol/L NK84 and the indicated concentrations of PS-341. Equal protein loading in each lane was verified by using an antibody directed against β -actin.



treatment with PS-341, whereas treatment with 10 μ mol/L NK84 does not lead to accumulation of poly-ubiquitinated proteins. However, simultaneous inhibition of proteasome and HDAC6 activity results in massive accumulation of poly-ubiquitinated proteins and cell toxicity (Fig. 5C, *left*). This suggests that although the HDAC6-dependent pathway is a minor protein degradation pathway under normal conditions, it becomes crucial in compensating for high levels of UPS stress generated by proteasomal inhibition in ovarian cancer cells. Surprisingly, although PS-341 treatment of IOSE-29 cells does trigger the accumulation of poly-ubiquitinated protein, simultaneous inhibition of proteasome and HDAC6 activity does not

further increase in levels of poly-ubiquitinated protein compared with PS-341 treatment alone (Fig. 5C, *right*). This finding and the failure of IOSE-29 cell to form aggresome-like structures even at higher level proteasome inhibition (20 nmol/L PS-341) both suggest that ovarian cancer cells and IOSEs differ in their capacity to form aggresomes after proteasome blockade and are consistent with the low level of HDAC6 expression in IOSE.

HDAC6 inhibition impedes cell spreading and migration of ovarian cancer cells. Pharmacologic inhibition of HDAC6 activity and knockdown of HDAC6 protein levels have been shown to hinder the motility of fibroblasts (23, 24), T-cells (25), and breast cancer cell lines (26). Because cell motility has clear

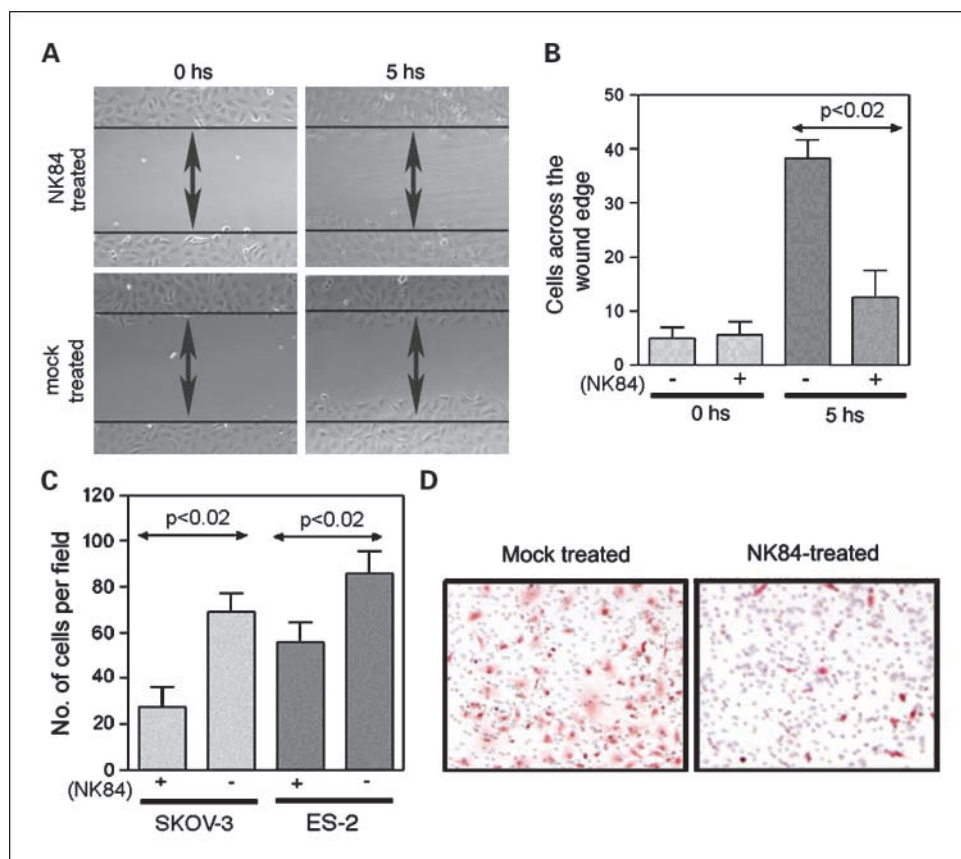


Fig. 6. Pharmacologic inhibition of HDAC6 impedes cell motility and migration of ovarian cancer cells. *A*, plates of confluent SKOV-3 cells either mock or NK84 treated (10 $\mu\text{mol/L}$) were examined by phase-contrast microscopy at the time of removal by scratching (0 h) and 5 h later. *B*, analysis of the number of SKOV-3 cells spreading across the wound; columns, mean of three independent experiments; bars, SD. *C*, an equivalent number (2.5×10^4) of SKOV-3 or ES-3 cells mock treated or treated with 10 $\mu\text{mol/L}$ of NK84 HDAC6 inhibitor were seeded in migration chambers, and migrating cells were counted per each condition 8 h thereafter. Three different fields of cells for each condition were counted at $\times 40$. Each assay was done in triplicate. Columns, mean of migrating cells per microscopic field; bars, SD. *D*, representative example of migration assay conducted on mock or NK84-treated SKOV-3 cells.

relevance to cancer cell invasion and metastasis, we assessed whether HDAC6 function is important for motility/migration of ovarian cancer cells. Immuno-staining analysis reveals that HDAC6 is mainly localized in punctate structures around the nuclei in nonmigrating cells, whereas it localizes in the leading edges of migrating ovarian cancer cells (Supplementary Fig. S3), suggesting a role for HDAC6 during ovarian cancer cell motility. To investigate the potential role for HDAC6 during cell movement, the effect of HDAC6 inhibition on ovarian cancer cell spreading was tested using scratch assays. As shown in Fig. 6A, spreading of SKOV-3 ovarian cancer cells across a gash in a monolayer occurs at a retarded rate upon NK84 treatment compared with mock treated cells (Fig. 6A and B).

We further investigated the effect of HDAC6 inhibition upon motility in a *trans*-Matrigel migration assay based on chemoattraction to higher serum levels. As shown in Fig. 6C, the ability of ES-2 and SKOV-3 ovarian cancer cell lines to invade the Matrigel substratum is inhibited in NK84-treated compared with control cells. A representative example of these *trans*-Matrigel migration assays with or without NK84 treatment is given in Fig. 6D. The rapid redistribution of HDAC6 during ovarian cancer cell motility and the retardation of movement by pharmacologic inhibition of HDAC6 deacetylase activity are consistent with its pivotal role in controlling the levels of cortactin (27) and acetylated α -tubulin in dynamic cellular structures (23, 24).

Discussion

In this study, we show that up-regulation of HDAC6 occurs in ovarian cancer cell lines and tissues likely in response

to UPS stress. Consistent with the hypothesis of higher demand for HDAC6 activity by ovarian cancer cells, the HDAC6-specific inhibitor NK84 selectively induces cytotoxicity in ovarian cancer cells while sparing IOSE cell lines. Importantly, we find that inhibition of HDAC6 synergistically enhances the cytotoxic effect caused by proteasomal inhibition in a UPS stress-dependent manner. Finally, we show that HDAC6 plays a critical role in ovarian cancer cell motility and migration.

As a result of a tightly regulated process necessary to maintain homeostasis, proteins within cells are constantly synthesized and then degraded via two pathways: the proteasomal and the lysosomal pathway. Importantly, the HDAC6-dependent lysosomal pathway seems to become a critical pathway for proteasomal degradation under circumstances of aberrant accumulation of aggregation-prone protein or upon inhibition of proteasome function, situations leading to increased and toxic levels of UPS stress.

We have previously shown that aberrant high expression of proteasomes naturally occurs in ovarian cancer *in vivo* and that their protein levels follow the demand/offers rule as they can be manipulated *in vitro* by changing the level of metabolic activity (5). In this report, we show that ovarian cancer cells also aberrantly express HDAC6 *in vivo* and *in vitro*, suggesting that the concomitant up-regulation of conventional and alternative protein degradation pathway may be required in ovarian cancer cells to ensure homeostasis. Other investigators have reported up-regulation of HDAC6 in oral squamous cell carcinoma (28), suggesting that this may be a common phenomenon. Further evidence for up-regulation of the alternate pathway in ovarian

cancer cells is provided by enhanced basal autophagic activity, their selective loss of viability upon HDAC6 inhibition (with and without concomitant proteasomal inhibition), and their propensity to form aggresomes upon proteasomal treatment compared with IOSE.

Specific small molecule inhibitors represent a powerful tool for investigating the effect of inhibition of HDAC6 in cancer setting (29–31). Indeed, Tubacin, the first HDAC6-specific inhibitor discovered, has been successfully evaluated for its antitumor activity in several cancer types, including multiple myeloma, pancreatic cancer, lung cancer, and breast cancer-derived cell lines (6, 13, 32). Our study extends these previous findings by showing that the cytotoxic effect of HDAC6 inhibition occurs in ovarian cancer cells while sparing their immortalized normal counterpart. Significantly, increased levels of acetylation of α -tubulin are already observable after only 8 hours of NK84 exposure (data not shown). This result confirms efficient and rapid inhibition of HDAC6 activity by NK84, whereas cytotoxicity requires prolonged exposure to HDAC6 inhibition.

Leading edges of cells are highly dynamic structures. Within eukaryotic cells, motility requires tight regulation of the levels of acetylated α -tubulin and cortactin. Various lines of

evidence indicate that HDAC6 also plays an important role in cell motility. Indeed, its effect on the levels of α -tubulin acetylation at the leading edges of fibroblasts ensures tight regulation of microtubule polymerization. Notably, overexpression of HDAC6 has been shown to promote chemotactic cell movement, and here we show that its activity is required for chemotaxis. These findings suggest that the combination therapy may have benefits beyond simply killing ovarian cancer cells, possibly by retarding metastatic spread. Efforts to determine the pharmacodynamics of HDAC6 inhibitors are under way with a view to preclinical testing of these hypotheses.

Disclosure of Potential Conflicts of Interest

No potential conflicts of interest were disclosed.

Acknowledgments

We thank the Tissue bank of the Johns Hopkins Specialized Programs of Research Excellence in Cervical Cancer for tissue specimens, Millenium Pharmaceuticals, Inc., for providing PS-341, Drs. Ivan Borrello and Kimberly Noonan for providing us with bone marrow aspirates, and Sean Patrick for her encouragement and fund raising activities.

References

- Ciechanover A. Intracellular protein degradation: from a vague idea thru the lysosome and the ubiquitin-proteasome system and onto human diseases and drug targeting. *Cell Death Differ* 2005;12:1178–90.
- Aghajanian C. Clinical update: novel targets in gynecologic malignancies. *Semin Oncol* 2004;31:22–6; discussion 33.
- Richardson PG, Mitsiades C, Hideshima T, Anderson KC. Proteasome inhibition in the treatment of cancer. *Cell Cycle* 2005;4:290–6.
- Rajkumar SV, Richardson PG, Hideshima T, Anderson KC. Proteasome inhibition as a novel therapeutic target in human cancer. *J Clin Oncol* 2005;23:630–9.
- Bazzaro M, Lee MK, Zoso A, et al. Ubiquitin-proteasome system stress sensitizes ovarian cancer to proteasome inhibitor-induced apoptosis. *Cancer Res* 2006;66:3754–63.
- Hideshima T, Bradner JE, Wong J, et al. Small-molecule inhibition of proteasome and aggresome function induces synergistic antitumor activity in multiple myeloma. *Proc Natl Acad Sci U S A* 2005;102:8567–72.
- Pandey UB, Batlevi Y, Baehrecke EH, Taylor JP. HDAC6 at the Intersection of Autophagy, the Ubiquitin-Proteasome System and Neurodegeneration. *Autophagy* 2007;3:643–5.
- Pandey UB, Nie Z, Batlevi Y, et al. HDAC6 rescues neurodegeneration and provides an essential link between autophagy and the UPS. *Nature* 2007;447:859–63.
- Iwata A, Riley BE, Johnston JA, Kopito RR. HDAC6 and microtubules are required for autophagic degradation of aggregated huntingtin. *J Biol Chem* 2005;280:40282–92.
- Hook SS, Orian A, Cowley SM, Eisenman RN. Histone deacetylase 6 binds polyubiquitin through its zinc finger (PAZ domain) and copurifies with deubiquitinating enzymes. *Proc Natl Acad Sci U S A* 2002;99:13425–30.
- Kawaguchi Y, Kovacs JJ, McLaurin A, et al. The deacetylase HDAC6 regulates aggresome formation and cell viability in response to misfolded protein stress. *Cell* 2003;115:727–38.
- Boyault C, Zhang Y, Fritah S, et al. HDAC6 controls major cell response pathways to cytotoxic accumulation of protein aggregates. *Genes Dev* 2007;21:2172–81.
- Nawrocki ST, Carew JS, Pino MS, et al. Aggresome disruption: a novel strategy to enhance bortezomib-induced apoptosis in pancreatic cancer cells. *Cancer Res* 2006;66:3773–81.
- Narasipura SD, Wojciechowski JC, Charles N, Liesveld JL, King MR. P-Selectin coated microtube for enrichment of CD34+ hematopoietic stem and progenitor cells from human bone marrow. *Clin Chem* 2008;54:77–85.
- Nimmanapalli R, Fuino L, Bali P, et al. Histone deacetylase inhibitor LAQ824 both lowers expression and promotes proteasomal degradation of Bcr-Abl and induces apoptosis of imatinib mesylate-sensitive or -refractory chronic myelogenous leukemia-blast crisis cells. *Cancer Res* 2003;63:5126–35.
- Guo F, Sigua C, Tao J, et al. Cotreatment with histone deacetylase inhibitor LAQ824 enhances Apo-2L/tumor necrosis factor-related apoptosis inducing ligand-induced death inducing signaling complex activity and apoptosis of human acute leukemia cells. *Cancer Res* 2004;64:2580–9.
- Chou TC, Talalay P. Quantitative analysis of dose-effect relationships: the combined effects of multiple drugs or enzyme inhibitors. *Adv Enzyme Regul* 1984;22:27–55.
- Stemson SM, Wong JC, Grozinger CM, Schreiber SL. Synthesis of 7200 small molecules based on a substructural analysis of the histone deacetylase inhibitors trichostatin and trapoxin. *Org Lett* 2001;3:4239–42.
- Bali P, Pranpat M, Bradner J, et al. Inhibition of histone deacetylase 6 acetylates and disrupts the chaperone function of heat shock protein 90: a novel basis for antileukemia activity of histone deacetylase inhibitors. *J Biol Chem* 2005;280:26729–34.
- Rodriguez-Gonzalez A, Lin T, Ikeda AK, et al. Role of the aggresome pathway in cancer: targeting histone deacetylase 6-dependent protein degradation. *Cancer Res* 2008;68:2557–60.
- Whitesell L, Mimnaugh EG, De Costa B, Myers CE, Neckers LM. Inhibition of heat shock protein HSP90-60v-src heteroprotein complex formation by benzoquinone ansamycins: essential role for stress proteins in oncogenic transformation. *Proc Natl Acad Sci U S A* 1994;91:8324–8.
- Rosenwald IB. The role of translation in neoplastic transformation from a pathologist's point of view. *Oncogene* 2004;23:3230–47.
- Tran AD, Marmo TP, Salam AA, et al. HDAC6 deacetylation of tubulin modulates dynamics of cellular adhesions. *J Cell Sci* 2007;120:1469–79.
- Hubbert C, Guardiola A, Shao R, et al. HDAC6 is a microtubule-associated deacetylase. *Nature* 2002;417:455–8.
- Cabrero JR, Serrador JM, Barreiro O, et al. Lymphocyte chemotaxis is regulated by histone deacetylase 6, independently of its deacetylase activity. *Mol Biol Cell* 2006;17:3435–45.
- Saji S, Kawakami M, Hayashi S, et al. Significance of HDAC6 regulation via estrogen signaling for cell motility and prognosis in estrogen receptor-positive breast cancer. *Oncogene* 2005;24:4531–9.
- Gao YS, Hubbert CC, Lu J, et al. Histone deacetylase 6 regulates growth factor-induced actin remodeling and endocytosis. *Mol Cell Biol* 2007;27:8637–47.
- Sakuma T, Uzawa K, Onda T, et al. Aberrant expression of histone deacetylase 6 in oral squamous cell carcinoma. *Int J Oncol* 2006;29:117–24.
- Haggarty SJ, Koeller KM, Wong JC, Grozinger CM, Schreiber SL. Domain-selective small-molecule inhibitor of histone deacetylase 6 (HDAC6)-mediated tubulin deacetylation. *Proc Natl Acad Sci U S A* 2003;100:4389–94.
- Wong JC, Hong R, Schreiber SL. Structural biasing elements for in-cell histone deacetylase paralog selectivity. *J Am Chem Soc* 2003;125:5586–7.
- Itoh Y, Suzuki T, Kouketsu A, et al. Design, synthesis, structure-selectivity relationship, and effect on human cancer cells of a novel series of histone deacetylase 6-selective inhibitors. *J Med Chem* 2007;22:5425–38.
- Marcus AI, Zhou J, O'Brate A, et al. The synergistic combination of the farnesyl transferase inhibitor lonafarnib and paclitaxel enhances tubulin acetylation and requires a functional tubulin deacetylase. *Cancer Res* 2005;65:3883–93.

Clinical Cancer Research

Ubiquitin Proteasome System Stress Underlies Synergistic Killing of Ovarian Cancer Cells by Bortezomib and a Novel HDAC6 Inhibitor

Martina Bazzaro, Zhenhua Lin, Antonio Santillan, et al.

Clin Cancer Res 2008;14:7340-7347.

Updated version	Access the most recent version of this article at: http://clincancerres.aacrjournals.org/content/14/22/7340
Supplementary Material	Access the most recent supplemental material at: http://clincancerres.aacrjournals.org/content/suppl/2008/11/14/14.22.7340.DC1

Cited articles	This article cites 32 articles, 18 of which you can access for free at: http://clincancerres.aacrjournals.org/content/14/22/7340.full#ref-list-1
Citing articles	This article has been cited by 11 HighWire-hosted articles. Access the articles at: http://clincancerres.aacrjournals.org/content/14/22/7340.full#related-urls

E-mail alerts	Sign up to receive free email-alerts related to this article or journal.
Reprints and Subscriptions	To order reprints of this article or to subscribe to the journal, contact the AACR Publications Department at pubs@aacr.org .
Permissions	To request permission to re-use all or part of this article, use this link http://clincancerres.aacrjournals.org/content/14/22/7340 . Click on "Request Permissions" which will take you to the Copyright Clearance Center's (CCC) Rightslink site.